THE JOURNAL OF COMPARATIVE NEUROLOGY 427:362–369 (2000)

Binocular Competition Does Not Regulate Retinogeniculate Arbor Size in Fetal Monkey

CARA J. WEFERS,[1] COLETTE DEHAY,[2] MICHEL BERLAND,[3] HENRY KENNEDY,[2] AND LEO M. CHALUPA[1]*

[1]Section of Neurobiology, Physiology and Behavior and Department of Ophthalmology, University of California, Davis, California 95616

[2]Institut National de la Sante et de la Recherche Medicale U371, Cerveau et Vision, 69500 Bron, France

[3]Faculte de Medecine Lyon SUD, Sevice Gynecologie Obstetrique, 69495 Pierre Benite Cedex, France

ABSTRACT

Binocular interactions play a prominent role in shaping the axonal arbors of geniculocortical fibers and the arbors of Y cells in the retinogeniculate pathway of the fetal cat. Fiber interactions between the two eyes have also been suggested to regulate the formation of retinal projections to the dorsal lateral geniculate nucleus (dlgn) of the fetal monkey, but whether this reflects structural refinements of retinal arbors has not been established. To address this issue, we quantified the morphologic properties of individual fibers in two macaque monkeys at embryonic day (E) 110 and E121 that had an eye removed at E69 and E61, respectively. Fibers were labeled by DiI crystals into the fixed optic tract and were visualized by confocal microscopy. Three measurements were made: the number of branch points within the axon terminal arbor, the total arborization length, and the incidence of axonal side branches on the preterminal axon within the confines of the geniculate. There were no significant differences with respect to these parameters between the prenatal enucleates and normal monkeys of comparable age. This was the case for retinal fibers innervating the magnocellular and the parvocellular segments of the dlgn. The arbors stemming from the remaining eye were widely distributed in the dlgn, with some terminating in territories normally innervated by the other (enucleated) eye. These results lend support to the hypothesis that the expanded projection from the remaining eye to the lateral geniculate nucleus of the prenatally enucleated monkey is due to the maintenance of a contingent of retinal fibers normally eliminated by ganglion cell death. J. Comp. Neurol. 427:362–369, 2000.

Indexing terms: retinogeniculate projections; primate; prenatal development; terminal arborization; monocular enucleation; binocular competition

In the developing visual system, the importance of competitive interactions between projections from the two eyes has been well recognized since Wiesel and Hubel (1963, 1965) first demonstrated the profound consequences of monocular deprivation on the formation of ocular dominance columns in the visual cortex. More recently, it has been shown that even brief periods of monocular occlusion are sufficient to cause geniculocortical arbors from the deprived eye to undergo a striking reduction in complexity and those from the nondeprived eye to expand markedly (Antonini and Stryker, 1993, 1996).

Binocular interactions have also been implicated in the formation of segregated left and right projections to the dorsal lateral geniculate nucleus (dlgn; for reviews, see

Grant sponsor: Institut de la Sante et de la Recherche Medicale; Grant sponsor: National Institutes of Health.

*Correspondence to: Dr. Leo M. Chalupa, Neurobiology Physiology & Behavior, University of California, Davis, CA 95616.
E-mail: lmchalupa@ucdavis.edu

Received 22 May 2000; Revised 1 August 2000; Accepted 1 August 2000

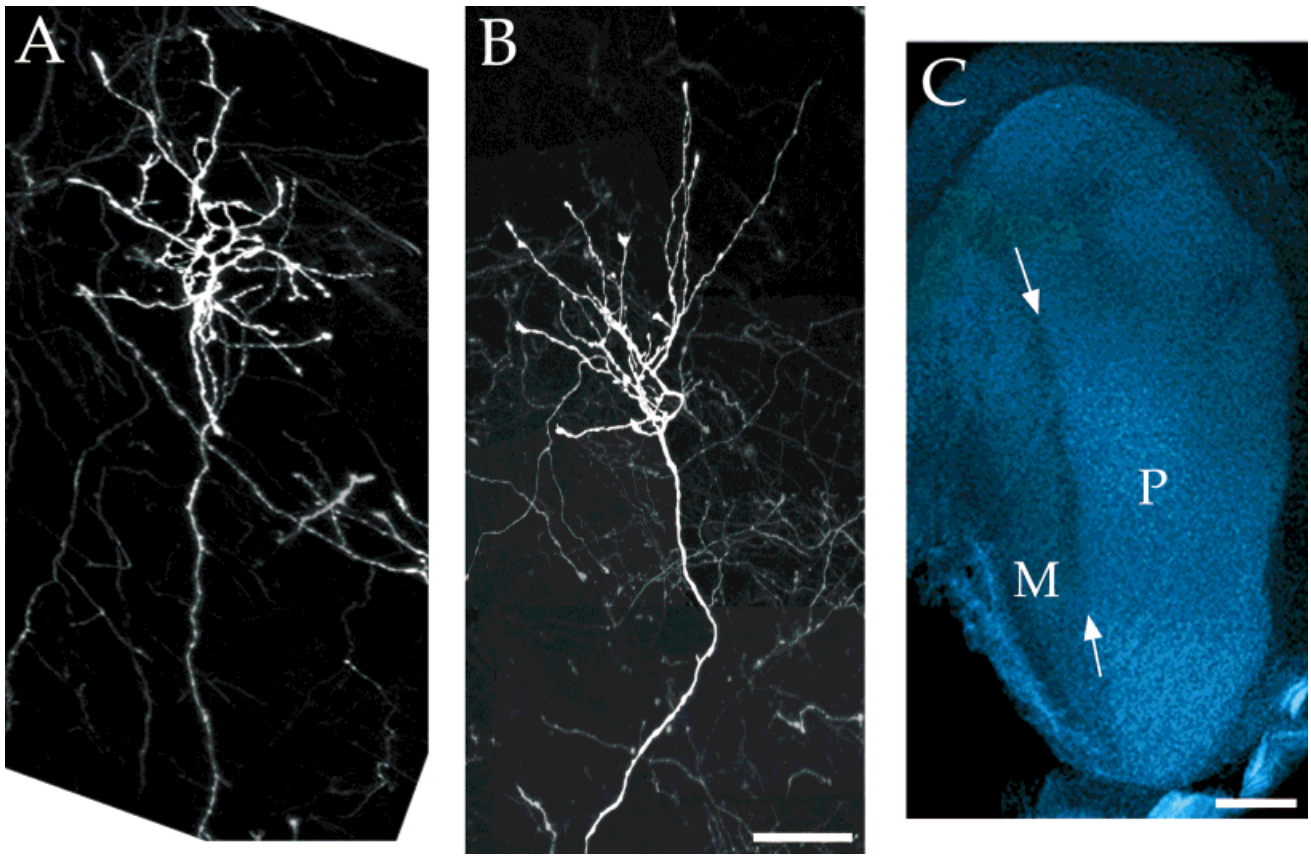

Fig. 1. Photomontages of arborizations. Confocal photomontages of retinogeniculate axons found in the magnocellular (**A**; M) and parvocellular (**B**; P) segments of the dorsal lateral geniculate nucleus (dlgn) of the enucleate. **C:** Confocal image of a 200-μm coronal section from the caudal portion of embryonic day 69 and 110 enucleate dlgn stained with bisbenzimide. Note the preservation of the M–P border (white arrows) even in the absence of eye-specific lamination. Scale bars = 50 μm in A,B; 250 μm in C.

Casagrande and Condo, 1988; Garraghty and Sur, 1993). Based on labeling patterns obtained after intraocular injection of anterograde tracers, it has been reported that the inputs from the two eyes in fetal cats and monkeys are initially intermingled in the dlgn before forming eye-specific layers (Rakic, 1976; Shatz, 1983). During this overlap period retinogeniculate fibers in the fetal cat are characterized by numerous side branches that innervate inappropriate ocular domains, and the subsequent withdrawal of these side branches has been suggested to account for the formation of eye-specific layers (Sretavan and Shatz, 1984, 1986). A role for binocular interactions in this process has been inferred from the finding that removal of one eye in the fetal cat results in the expansion of Y-cell retinogeniculate arbors, with some Y cells innervating territory normally occupied by left and right eye inputs (Garraghty et al., 1988, 1998). The dimensions of X-type arbors appear normal in prenatally enucleated cats, but some X-type arbors innervate regions of the dlgn normally occupied by the other (enucleated) eye. Presumably, during normal development, these inappropriately positioned X inputs are eliminated by retinal ganglion cell loss (Chalupa et al., 1984; Williams et al., 1986). Thus, in the fetal cat, binocular interactions appear to regulate the dimensions of Y retinogeniculate arbors, whereas the size of the X arbors appears to be established independent of this process.

In contrast to the case in the fetal cat, very few axonal side branches are present on monkey retinogeniculate fibers before and after eye-specific projections have been established (Snider et al., 1999). In the mature monkey, it is also the case that the two major ganglion cell classes, Pα and Pβ, project to different sets of dlgn layers; in the cat, X and Y inputs are intermingled within the main dlgn laminae (Jones, 1985). The distinct features of retinal projections in the developing and mature monkey prompted us to consider whether binocular interactions are involved in shaping primate retinogeniculate arbors, as has been found for Y cells in fetal cats. To address this issue, we examined the morphologic properties of retinogeniculate axons in fetal monkeys that had one eye removed during the period of maximum binocular overlap. These findings were compared with the retinal arbors of normal fetal monkeys studied at an equivalent age (Snider et al., 1999). Both magnocellular (M) and parvocellular (P) arbors were found to develop normally in the absence of binocular interactions, although some retinal terminals were distributed in dlgn territories normally occupied by fibers from the other (enucleated) eye.

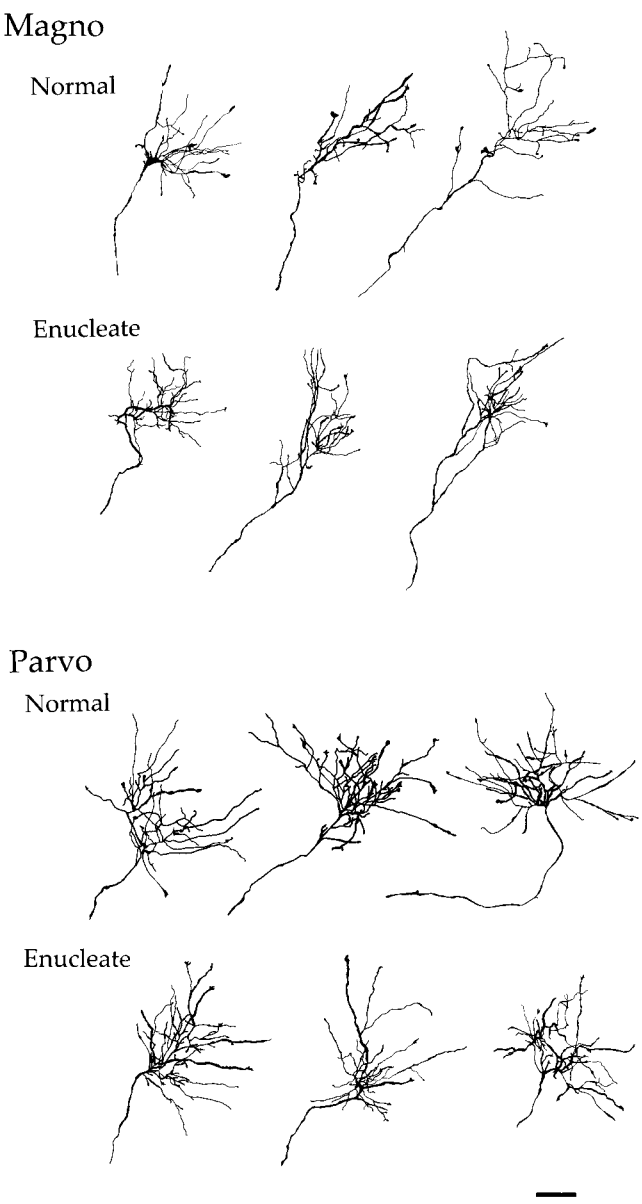

Fig. 2. Tracings of confocal montages. Tracings of reconstructed confocal photomontages of retinogeniculate terminal arbors in the normal (embryonic day 112) and enucleated (embryonic days 61 and 121) fetal monkey. Representative magnocellular (magno) and parvocellular (parvo) arborizations are shown. Arbors from both magnocellular and parvocellular segments in the enucleate resemble their normal counterparts. Scale bar = 50 μm.

MATERIALS AND METHODS

All procedures involving animal use were approved by institutional Animal Care and Use Committees (INSERM and University of California, Davis). Monocular enucleations were performed on two fetal cynomologus monkeys of known gestational ages at embryonic day (E) 61 and E69 (full term is 165 days). Timed-pregnant monkeys were prepared for surgery under Alfatesine anesthesia. After intubation, anesthesia was continued with halothane in an N_2O:O_2 (70:30) mixture. A detailed description of the enucleation procedure has been published (Dehay et al., 1996). In short, a midline abdominal incision was made, uterotomy was performed, the fetal head was exposed, one eye was removed, and the fetus was placed back in the uterus. Vital signs were monitored throughout the procedure. All incisions were sutured, and the animal was medicated with an analgesic (Visceralgine intramuscularly) before being returned to its cage. Visceralgine was continued twice daily for 48 hours. The fetuses were delivered by cesarean section at E121 and E110, respectively, deeply anesthetized with barbiturate (1 ml injected intraperitoneally), and perfused transcardially with 0.9% saline followed by 4% paraformaldehyde fixative.

Fiber labeling and histology

A small block of tissue including the optic tract and dlgn was isolated and embedded in 5% agar. The block was then sectioned in the coronal plane on a Vibratome until the optic tract close to the dlgn was visible, and two small crystals of 1,1′-dioctodecyl-3,3,3′3′tetramethylinodocarbocyanine perchlorate (DiI; Molecular Probes, Eugene, OR) were implanted into the tract. Subsequently, the block was submerged in 4% paraformaldehyde and stored in the dark at 37°C to allow for passive diffusion of the DiI to the dlgn. After 1–4 months, the dlgn was sectioned coronally at 200 μm, mounted on gelatinized slides, stained with 0.005% bisbenzimide to visualize the outline of the dlgn, and coverslipped.

Analysis

Labeled retinogeniculate axons were examined using a Bio-Rad MRC-600 confocal microscope system (Bio-Rad, Richmond, CA) equipped with an argon laser mounted on an Olympus microscope, a Bio-Rad MRC-2400 confocal system with an argon and a krypton laser, or a Leica confocal microscope (Leica, Deerfield, IL) with an argon, krypton, and ultraviolet laser. An Olympus D Planapo UV 40× objective (numerical aperture = 0.85) or a Leica Planapo 5× objective (numerical aperture = 0.15) was used to collect optical sections in a sequence as a function of tissue depth (150–200 μm) by mechanically choosing the position of the microscope stage along the z axis and recording an image at 2-μm intervals at 40× (5 μm at 5×) to generate a z series. Images of 768 × 512 pixels were generated. Those images were then compiled, and the z series was projected to obtain a view that was in focus throughout the entire labeled area. Photographic montages of retinogeniculate axons were constructed with several z-series projections (Adobe Photoshop 4.0) and printed with a Fujix Pictography 3000 printer.

Measurements of terminal arbors, branch points within terminal arbors, and number of side branches along the parent axon were calculated from confocal montages of retinogeniculate axons from various loci within the dlgn. Using Imagespace software, total terminal arbor lengths were calculated by measuring and adding all axon segments belonging to the terminal arborization. The number of side branches per millimeter of parent axon was calculated using NIH Image software.

Reconstruction of arbor loci within the dlgn

Camera lucida drawings of coronal sections of the dlgns contralateral and ipsilateral to the intact eye were made, and the position of each labeled arbor was plotted on these drawings. To obtain a schematic representation of the

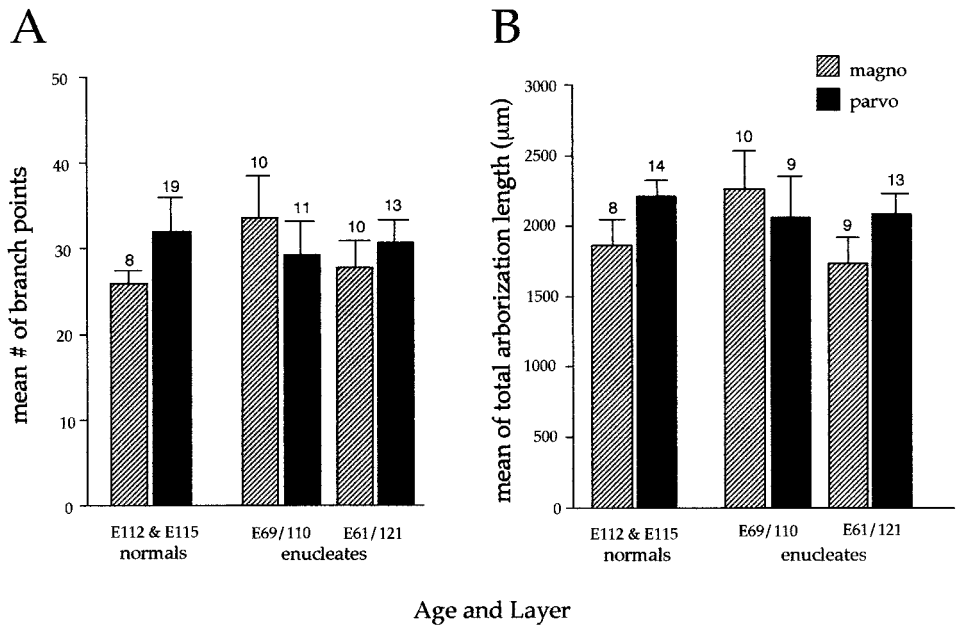

Fig. 3. Measurements of terminal arborizations. Analysis of terminal arborization complexity of single retinogeniculate axons in magnocellular (stippled bars) and parvocellular (solid bars) layers in the normal and enucleated animal. **A:** Mean number of branch points. **B:** Mean total length of axon contributing to the terminal arbor. The number of arbors analyzed is indicated on top of each bar, and the vertical brackets denote the standard error of the mean. Normals include data from one embryonic day 112 animal and one embryonic day 115 animal from previous studies (Meissirel et al., 1997; Snider et al., 1999).

distributions of these arbors, a three-dimensional serial section reconstruction and solid modeling of the sections was performed using Neurolucida software (MicroBrightField, Inc. Colchester, VT). The contralateral and ipsilateral dlgns were combined to depict the crossed and uncrossed fibers in a single reconstruction. For illustrative purposes, the data from the two animals were combined. For this reason, sections from the E110 monkey were enlarged to approximate those of the E121 monkey. The three-dimensional model could be rotated in different planes to allow visualization of arbor positions from all perspectives.

RESULTS

The results are based on the analysis of 44 fibers from two fetal monkeys that had one eye removed at an early stage of gestation. One of these animals was monocularly enucleated at E69 and killed at E110, and the other underwent these procedures at E61 and E121. For comparison, 27 retinogeniculate fibers from two normal animals (one at E112 and one at E115) are included from previous studies (Meissirel et al., 1997; Snider et al., 1999). As was the case in our previous studies, the fibers analyzed were considered to be completely labeled when numerous growth cones and distal filopodia of very fine caliber were present (Fig 1A,B). For every fiber, we distinguished between terminal arbors that were confined to the M or P regions of the dlgn. The laminar boundary between these regions was already evident (Fig. 1C) in the caudal portion of the nucleus by E110 (see Fig. 1C of Rakic, 1981).

To provide an overall view of M and P retinogeniculate terminal arbors in normal and prenatally enucleated animals, tracings of reconstructed photomontages (such as those shown in Fig. 1A,B) are depicted in Figure 2. The terminal arbors found in the enucleated monkeys did not differ from those in normal monkeys, and at this age there were no appreciable differences between M and P arbors.

These observations were supported by a quantitative assessment of arbors that involved measurements of the number of branch points (Fig. 3A) as well as total arborization length (Fig. 3B). For both measures the differences between normal animals and each prenatal enucleate as well as between the two enucleates were found not to be statistically significant ($P > 0.05$ on a t-test).

Another morphologic feature examined was the incidence of axonal side branches on retinogeniculate axons. Axonal side branches are processes on the preterminal axon within the confines of the dlgn (Meissirel et al., 1997; Snider et al., 1999). As we showed previously, there are very few axonal side branches on retinogeniculate fibers throughout the prenatal development of macaque monkey (Snider et al., 1999). Figure 4 illustrates that such axonal processes are also few in number in prenatally enucleated monkeys. This was the case for both M and P axons.

To gain a better appreciation of the dimensions of retinogeniculate terminal arbors in the prenatally enucleated animals relative to the M and P segments of the dlgn, Figure 5 shows drawings of two such fibers in a cross section of the geniculate. The boundary between M and P is clearly evident in this caudal portion of the nucleus, but no eye-specific laminae are present. All fibers reconstructed in the vicinity of the M–P laminar boundary (n = 5) had their terminal arbors confined to either the M or P segments of the dlgn, as shown in Figure 5.

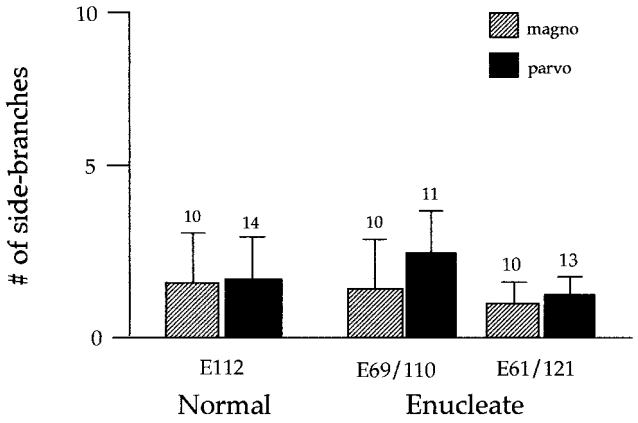

Fig. 4. Number of side branches. Graph comparing the number of side branches per millimeter of axon per fiber in normal and enucleated monkeys (magnocellular, stippled bar; parvocellular, solid bar). The number of axons analyzed is indicated on top of each bar, and the vertical brackets denote the standard error of the mean. For each length of axon, the total number of side branches was counted and divided by the total axon length. In the monkey, side branches on both parvocellular and magnocellular retinogeniculate axons, in the normal and the enucleated monkey, were few in number and relatively short.

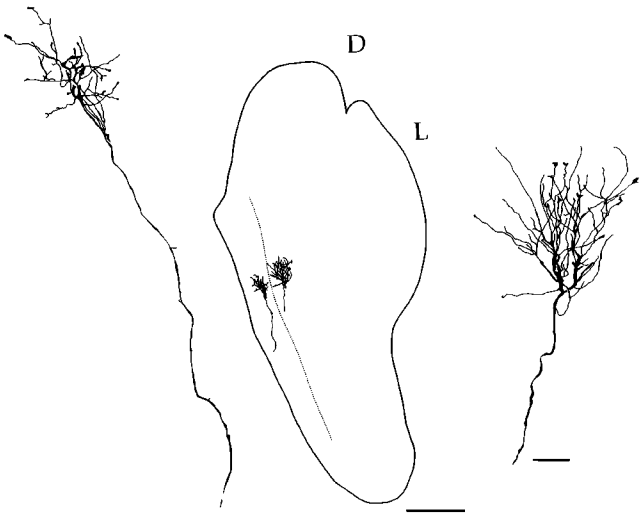

Fig. 5. Terminal arbors in relation to the dorsal lateral geniculate nucleus (dlgn). Drawing of a 200-μm coronal section through the posterior pole of the dlgn shows loci of reconstructed retinogeniculate axons in the enucleated monkey. The magnocellular–parvocellular border is designated by the stippled line. The terminal arbors are confined within the magnocellular and parvocellular segments. D, dorsal; L, lateral. Scale bars = 500 μm for section, 50 μm for enlarged individual axons.

Because eye-specific layers are absent in prenatally enucleated monkeys, we could not assign individual retinal arbors to territories within the dlgn normally innervated by one or the other retina. However, there was no indication of laminarlike clusterings of retinal arbors in the dlgn contralateral or ipsilateral to the remaining eye (Fig. 6). The widespread distribution of retinal arbors shown in Figure 6 would be expected if the remaining eye

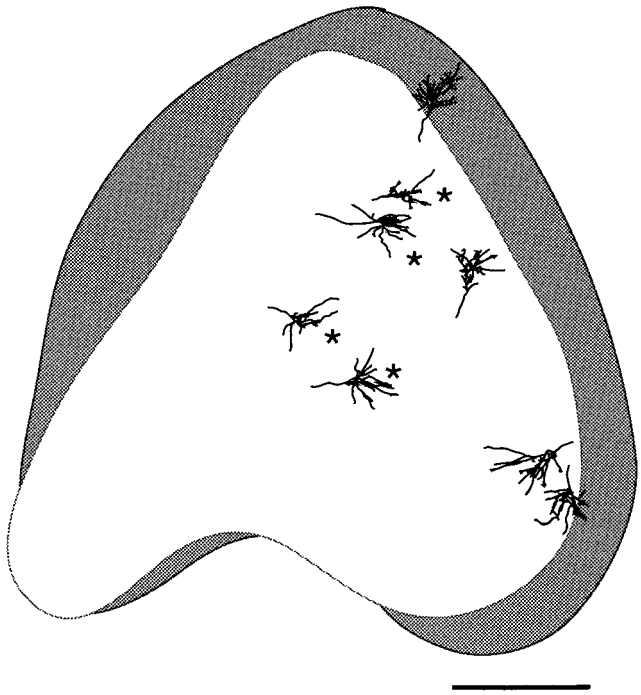

Fig. 6. A contingent of retinal arbors in the dorsal lateral geniculate nucleus (dlgn). Camera lucida drawings showing retinal arbors localized to two adjacent sections (each 200 μm thick) of the dlgn ipsilateral to the remaining eye. The more caudal section is denoted by shadings, and the arbors in the more rostral section are denoted with asterisks. Based on their position in the nucleus, these were positioned in the parvocellular segment. Note the relatively continuous distribution pattern in the dorsal–ventral axis and the absence of laminarlike gaps in the labeling pattern. Scale bar = 500 μm

had innervated territories normally reserved for the eye removed at an earlier stage of development. A continuous labeling pattern could also be observed in individual sections that contained multiple retinal arbors. In the example shown in Figure 7, the contingent of ipsilateral retinal fibers is distributed in a dorsal–ventral extent, spanning the parvocellular segment of the dlgn without prominent gaps. Because the dlgn is located in its usual position and is normal in size and shape in these prenatal enucleates (cf. Rakic, 1981), some of these ipsilateral fibers must have innervated territories normally occupied by the other eye.

DISCUSSION

We have quantified the morphologic features of single retinogeniculate fibers within the M and P segments of the dlgn in two fetal monkeys that had an eye removed at an earlier stage of gestation. The enucleations were performed at E61 and E69, during the period when the projections from the two eyes have been reported to be totally overlapping (Rakic, 1976, 1981). These enucleates were harvested at E121 and E110, respectively, a developmental period when eye-specific projections are normally established in the macaque monkey (Rakic, 1976, 1981). We found that the arbors of M and P fibers in the prenatal enucleates were not significantly different than normal in terms of the number of branch points within the terminal arbor, total length of axon contributing to the arbor, and

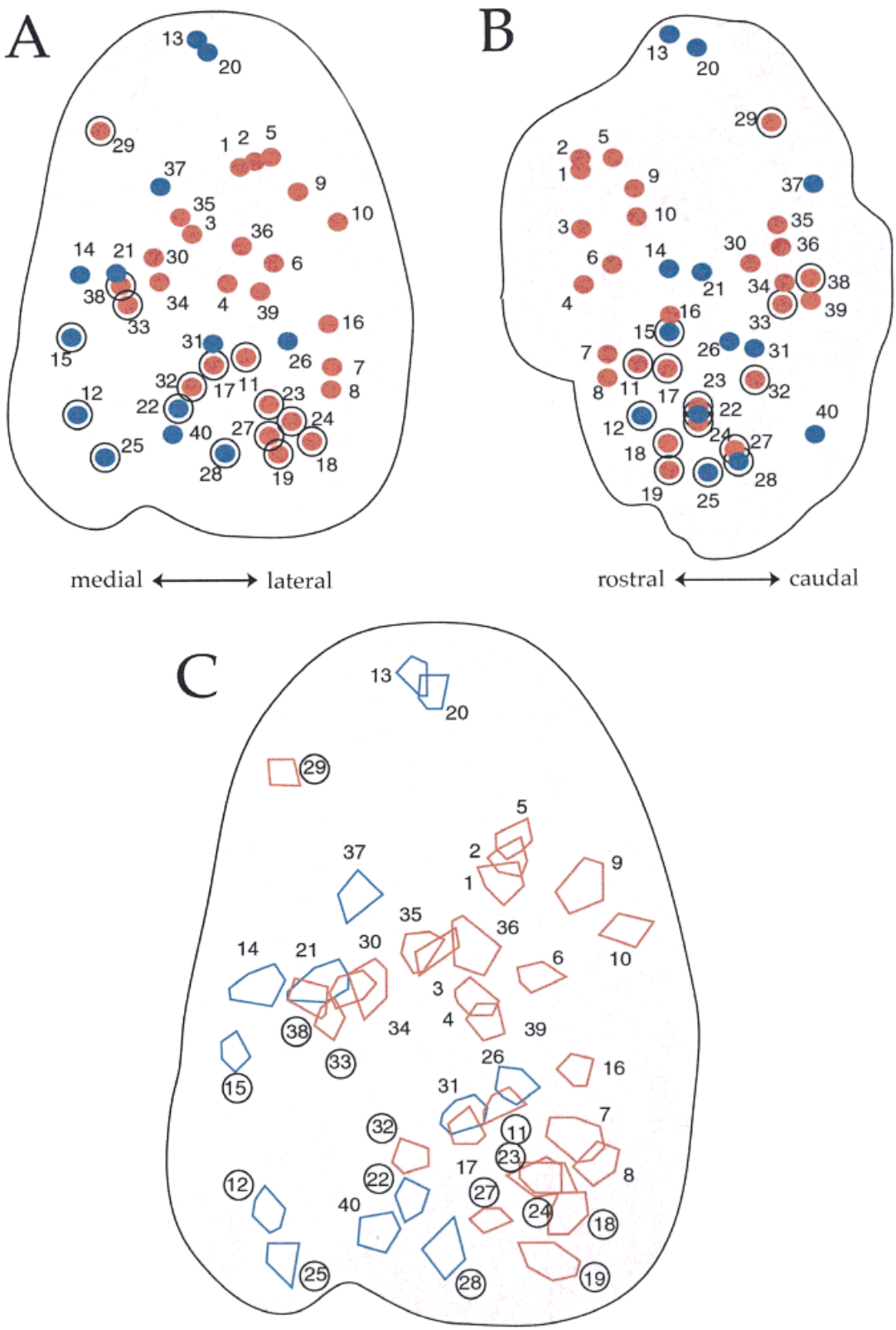

Fig. 7. Terminal arbor placement in the dorsal lateral geniculate nucleus (dlgn). Coronal (**A,C**) and lateral (**B**) views taken from a three-dimensional reconstruction of the dlgn. In A and B, blue and red dots represent the positions of DiI-labeled terminal arbors in the contralateral and ipsilateral dlgn, respectively, to the remaining eye. Both sets of inputs are widely distributed throughout the dlgn. In C, these colors represent the extent of each arbor in a coronal view. Numbers indicate the position of the arbors from rostral (1) to caudal (40) for the 40 fibers. Four other fibers quantified in this study are not included because these were lost due to fading. The circles around dots in A and B and around numbers in C indicate terminal arbors in the magnocellular segment of the dlgn. For the orientation of magnocellular and parvocellular layers in relation to the rostral–caudal extent of the fetal monkey dlgn, see Rakic (1977), in particular Figure 3 and Plate 1.

the number of side branches on the parent axon. Some M and P arbors, however, were located in territories within the dlgn that would have been innervated by the enucleated eye.

Before considering the implications of these observations, it is important to address some possible limitations of this study. One potential problem is that DiI in fixed tissue may not fill the entire terminal arbor. We believe that the labeling of the fibers studied was complete because of the fine morphologic details that were evident in our material, including numerous filopodia protruding from the distal ends of growth cones and the fine-caliber axonal side branches (see Fig. 2 of Snider et al., 1999). Also pertinent to this matter is the fact that identical methods showed an incidence of axonal side branches in the fetal cat (Snider et al., 1999) equivalent to what was obtained after in vitro labeling of retinogeniculate fibers by deposits of horseradish peroxidase into the optic tract (Sretavan and Shatz 1984, 1986). Another potential limitation is that the animals may not have been allowed to survive for a long enough period to observe an expansion of terminal arbors. We think that this is not the case because eye-specific retinogeniculate inputs are formed in the fetal monkey during the survival period used in this study (Rakic, 1976, 1981). Moreover, retinal arbors manifest marked growth and elaboration during this developmental period (Meissirel et al., 1997; Snider et al., 1999). Finally, it should be noted that the distinction made between M and P fibers is based on the territories innervated by these retinal axons within the developing dlgn. Thus, we cannot rule out the possibility that some of the fibers classified as stemming from one or the other retinal cell class may have innervated functionally inappropriate layers of the dlgn, but this would not alter the main conclusions of the present study.

The morphologic properties of single retinogeniculate fibers in fetal and in prenatally enucleated animals have been examined in detail in the cat (Sretavan and Shatz, 1984, 1986; Garraghty et al., 1988, 1998) and in the monkey (Snider et al., 1999; present study). The available evidence indicates clear-cut developmental differences between these two highly binocular species. In the fetal cat, retinal fibers are characterized by a high incidence of axonal side branches when projections from the two eyes are intermingled, and the loss of such exuberant processes appears to coincide with the formation of segregated projections (Sretavan and Shatz, 1984, 1986). In contrast, retinogeniculate fibers in the macaque monkey show continued growth and elaboration throughout the period of binocular overlap and during the subsequent formation of eye-specific domains. Moreover, the incidence of axonal side branches is negligible throughout fetal development, and this is the case for both M and P fibers (Snider et al., 1999).

Some Y-cell arbors undergo a marked expansion after the removal of one eye in the fetal cat, even though the dimensions of X-cell arbors develop normally (Garraghty et al., 1988, 1998). In the fetal monkey, both M and P retinogeniculate arbors form normally in the absence of binocular interactions. Thus, M, P, and X retinal fibers appear to be characterized by similar intrinsic programs that shape their terminal arbors, whereas the development of Y fibers is constrained by binocular interactions. What accounts for such differences among retinal fibers is unknown, and in this respect information about other cell classes could prove insightful. It should be noted that we have not included K cells in our analysis because these fibers, which normally innervate the interlaminar zones of the primate dlgn (Lachica and Casagrande, 1988), could not be distinguished from the overall sample. To our knowledge, the prenatal development of the cat's W retinogeniculate pathway also remains to be studied.

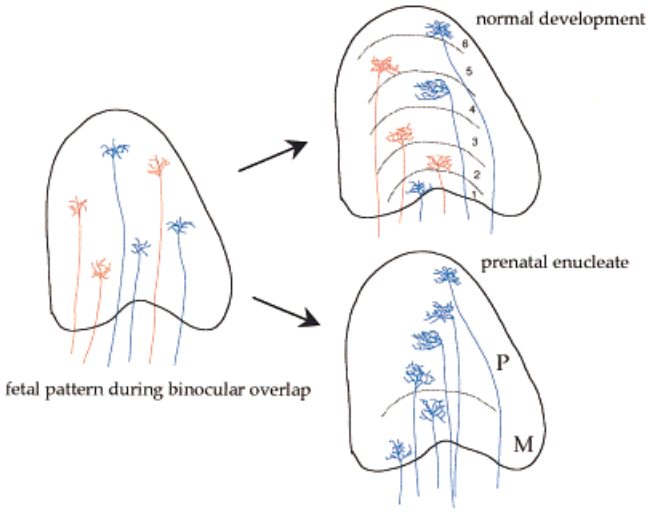

Fig. 8. Model of developmental pattern. The black outline represents a coronal section of the dorsal lateral geniculate nucleus (dlgn). The blue lines represent contralateral projections; ipsilateral projections are shown in red. On the left, a schematic of the fetal pattern is represented. During normal development, eye-specific layers are formed and inappropriate projecting axons are lost (top right.) After prenatal monocular enucleation, projections from the remaining eye are maintained, and this results in a widespread projection throughout the dlgn.

A developmental model of binocular overlap and segregation

More than two decades ago, Rakic (1976, 1981) demonstrated, by means of intraocular injections of tritiated amino acids, that the projections from the two eyes are initially intermingled within the dlgn of fetal monkeys and that monocular enucleation results in the maintenance of a widespread projection from the remaining eye. Similar observations have been reported in a number of different species (cat: Chalupa and Williams, 1984; for review, see Chalupa and Dreher, 1991). Several lines of evidence, including the results of the present study, suggest that in the monkey the initial overlap of left and right eye retinogeniculate projections and the widespread projection observed after fetal eye removal could be accounted for by the cellular events depicted schematically in Figure 8.

Retinogeniculate arbors show no exuberant growth in the fetal monkey, which suggests that restructuring of axon terminals does not play a role in the segregation of left and right eye projections (Snider et al., 1999). A massive loss of ganglion cells normally occurs in the fetal monkey during the binocular segregation period (Rakic and Riley, 1983a), and removal of one eye results in a significant increase in the number of fibers in the remaining optic nerve (Rakic and Riley, 1983b). As shown in the

present study, the dimensions of terminal arbors and the number of axonal side branches on retinogeniculate fibers are no different than normal in prenatally enucleated monkeys. The present findings suggest that some M and P fibers innervate territories normally occupied by the other eye. Such aberrantly positioned fibers are presumably eliminated during normal development by activity-mediated events (Scheetz et al., 1995; Penn et al., 1998).

The present observations differ in certain key respects from what has been described in the fetal cat. It is also the case that different primate species are characterized by differences in the organization of the retinal projections (Walls, 1953). For instance, in the squirrel monkey, there is considerable intermingling of left and right eye inputs to the P layers of the dlgn (Horton and Hocking, 1996). Thus, the degree to which this schema for the macaque monkey reflects a general developmental plan for the primate visual system remains to be established. Nevertheless, it seems reasonable to think that the present results have implications for the events occurring during the formation of the human visual system.

LITERATURE CITED

Antonini A, Stryker MP. 1993. Rapid remodeling of axonal arbors in the visual cortex. Science 260:1819–1821.

Antonini A, Stryker MP. 1996. Plasticity of geniculocortical afferents following brief or prolonged monocular occlusion in the cat. J Comp Neurol 369:64–82.

Casagrande VA, Condo GJ. 1988. Is binocular competition essential for layer formation in the lateral geniculate nucleus? Brain Behav Evol 31:198–208.

Chalupa LM, Dreher B. 1991. High precision systems require high precision "blueprints": a new view regarding the formation of connections in the mammalian visual system. J Cogn Neurosci 3:209–219.

Chalupa LM, Williams RW. 1984. Organization of the cat's lateral geniculate nucleus following interruption of prenatal binocular competition. Hum Neurobiol 3:103–107.

Chalupa LM, Williams RW, Henderson Z. 1984. Binocular interaction in the fetal cat regulates the size of the ganglion cell population. Neuroscience 12:1139–1146.

Dehay C, Giroud P, Berland M, Killackey HP, Kennedy H. 1996. Phenotypic characterization of respecified visual cortex subsequent to prenatal enucleation in the monkey: development of acetylcholinesterase and cytochrome oxidase patterns. J Comp Neurol 376:386–402.

Garraghty PE, Sur M. 1993. Competitive interactions influencing the development of retinal axonal arbors in cat lateral geniculate nucleus. Physiol Rev 73:529–545.

Garraghty PE, Shatz CJ, Sretavan DW, Sur M. 1988. Axon arbors of X and Y retinal ganglion cells are differentially affected by prenatal disruption of binocular inputs. Proc Natl Acad Sci USA 85:7361–7365.

Garraghty PE, Roe A, Sur M. 1998. Specification of retinogeniculate X and Y arbors in cats: fundamental differences in developmental programs. Brain Res Dev Brain Res 107:227–231.

Horton JC, Hocking DR. 1996. Anatomical demonstration of ocular dominance columns in striate cortex of the squirrel monkey. J Neurosci 16:5510–5522.

Jones EG. 1985. The thalamus. New York and London: Plenum Press.

Lachica EA, Casagrande VA. 1988. Development of primate retinogeniculate axon arbors. Vis Neurosci 1:103–123.

Meissirel C, Wikler KC, Chalupa LM, Rakic P. 1997. Early divergence of magnocellular and parvocellular functional subsystems in the embryonic primate visual system. Proc Natl Acad Sci USA 94:5900–5905.

Penn AA, Fiquelme PA, Feller MB, Shatz CJ. 1998. Competition in retinogeniculate patterning driven by spontaneous activity. Science 279: 2108–2112.

Rakic P. 1976. Prenatal genesis of connections subserving ocular dominance in the rhesus monkey. Nature 261:467–471.

Rakic P. 1977. Genesis of the dorsal lateral geniculate nucleus in the rhesus monkey: site and time of origin, kinetics of proliferation, routes of migration and pattern of distribution of neurons. J Comp Neurol 176:23–52.

Rakic P. 1981. Development of visual centers in the primate brain depends on binocular competition before birth. Science 214:928–931.

Rakic P, Riley KP. 1983a. Regulation of axon numbers in the primate optic nerve by prenatal binocular competition. Nature 305:135–137.

Rakic P, Riley KP. 1983b. Overproduction and elimination of retinal axons in the fetal rhesus monkey. Science 209:1441–1444.

Scheetz AJ, Williams RW, Dubin MW. 1995. Severity of ganglion cell death during early postnatal development is modulated by both neuronal activity and binocular competition. Vis Neurosci 12:605–610.

Shatz CJ. 1983. The prenatal development of the cat's retinogeniculate pathway. J Neurosci 3:482–499.

Snider CJ, Dehay C, Berland M, Kennedy H, Chalupa LM. 1999. Prenatal development of retinogeniculate axons in the macaque monkey during segregation of binocular inputs. J Neurosci 19:220–228.

Sretavan DW, Shatz CJ. 1984. Prenatal development of individual retinogeniculate axons during the period of segregation. Nature 308:845–848.

Sretavan DW, Shatz CJ. 1986. Prenatal development of retinal ganglion cell axons: segregation into eye-specific layers within the cat's lateral geniculate nucleus. J Neurosci 6:234–251.

Walls GL.1953. The lateral geniculate nucleus and visual histophysiology. Univ Calif Publ Physiol 9:1–100.

Wiesel T, Hubel DH. 1963. Effects of visual deprivation on morphology and physiology of cells in the cat's lateral geniculate body. J Neurophysiol 26:978–993.

Wiesel T, Hubel DH. 1965. Comparison of the effects of unilateral and bilateral eye closure on cortical unit responses in kittens. J Neurophysiol 28:1029–1040.

Williams RW, Bastiani MJ, Lia BL, Chalupa LM. 1986. Growth cones, dying axons and developmental fluctuations in the fiber population of the cat's optic nerve. J Comp Neurol 246:32–69.